IJE TRANSACTIONS B: Applications Vol. 34, No. 05, (May 2021) 1176-1183

International Journal of Engineering

Journal Homepage: www.ije.ir

Effect of Hydrodynamic Pressure on Saturated Sand Supporting Liquid Storage Tank During the Earthquake

A. A. Hussein*, M. A. Al-Neami, F. H. Rahil

Civil Engineering Department, University of Technology, Baghdad, Iraq

PAPER INFO

Paper history:
Received 10 February 2020
Received in revised form 10 April 2021
Accepted 12 April 2021

Keywords:
Hydrodynamic Pressure
Liquid Storage Tank
Earthquake
Acceleration Range

ABSTRACT

This paper aims to illuminate the influence of hydrodynamic pressure generated in a water storage tank on the behavior of saturated sand that its support. Experimental tests were performed on two cylindrical water tank models using a fabricated shaking table which consists of a flexible laminar shear box. The first model is a water storage tank partially full of water, and the second one is a tank model with an equivalent load of water pressure to simulate the water storage tank without hydrodynamic pressure. Three earthquake histories (Kobe, El-Centro, and Ali Al Gharbi) were implemented on models to study a varied range of acceleration. It was found that the settlement and lateral displacement directions in the water storage tank were significantly increased compared to the equivalent load resulted in the second model in all cases of the acceleration histories. Also, it was monitored the pore water pressure during the testing period, and it was noticed that the excess pore pressures were affected by the hydrodynamic pressure and increased compared to the results recorded at the condition of no hydrodynamic pressure.

doi:*10.5829/ije.2021.34.05b.11*

1. INTRODUCTION

The soil-structure interaction and fluid-structure interaction are independently composite occurrences for structures. Indeed, the dynamic characteristics of transient excitations and response of liquid storage tanks are directed by several features: the interaction among the fluid and the structure, earthquake characteristics, and the structure-soil interaction along with their boundaries. Kianoush and Ghaemmaghami [1] considered the soil structure-interaction influence on a storage tank for six types of soil. In dynamic behavior, the liquid tank-soil system was found to be associated with earthquake frequency. Chaduvulaa et al. [2] carried out shake table tests on the cylindrical storage steel elevated water tank with a scale model of 1:4. They found that the moment and base shear for impulsive value were increased with the increasing acceleration of the earthquake and decreased by increasing the angle of motion. Chaithra et al. [3] modeled the soil, tank, and fluid using finite elements to consider the soil flexibility influence with three types of soil with various flexibility on a tank wall filled with fluid to consider the structure-soil interaction influence. It was determined that soil flexibility considerably influences the reaction of the storage tank. Kotrasová [4] made a theoretical experience for the analytical calculation of hydrodynamic pressures and circular frequencies developed in rectangular liquid tanks during an earthquake. Analytical investigations of natural frequencies are compared with experimental ones. Chougule et al. [5] considered the earthquake implement of the base held a storage tank sitting on the soil having the tank wall mass, the roof mass, the base slab mass, and the water mass. It was concluded that under the effect of seismic forces with raising relation of maximum water depth to the tank diameter, the further water mass would motivate in the mode of impulsive while reducing water depth to tank diameter; further, the water mass will motivate in the mode of convective. Sadek et al. [6] considered a shallow rectangular storage tank's performance during an earthquake was taking into account fluid soil-structure

*Corresponding Author Institutional Email: 42080@student.uotechnology.edu.iq (A. A. Hussein)

Please cite this article as: A. A. Hussein, M. A. Al-Neami, F. H. Rahil, Effect of Hydrodynamic Pressure on Saturated Sand Supporting Liquid Storage Tank During the Earthquake, International Journal of Engineering, Transactions B: Applications Vol. 34, No. 05, (2021) 1176-1183

interaction that was modeled using 3D finite elements. It was determined that the dynamic's attitude on the storage tank is related to the frequency field of the soil movement. Hussein et al. [7] studied a cylindrical storage tank on medium and dense sand with different relative densities. It was found that the characteristic of soil and hydrodynamic pressure have a significant influence on the tank settlement, lateral displacement in (X and Z)-direction, and lateral soil stresses that are initialized due to the movement of the storage tank. Besides, the tank displacements have a considerable impact on the frequency field and frequency value.

Waghmare et al. [8] considered a numerical investigation in a multi-real earthquake for reinforced concrete elevated tanks in viscous dampers. They found that viscous dampers' nonlinearity and low damping constant contributed a comparable reduction to those viscous dampers with linear and high damping constant. Pan and Jiang [9] investigated the change in the reflection and distribution of earthquake waves at the surface interaction of layers. It proposed an enhanced method of the same input load usual viscous-spring simulated boundary model. Considered by the three approaches are variable, which illustrate that the uniform model of footing and the conventional corresponding input load of the earthquake wave can not represent the earthquake force correctly. Dram et al. [10] investigated the possible ability to use recycled tyre pieces as a compressible insertion right back retaining walls during dynamic load; it estimated the influence of thickness in a cushion that compressible angle of friction in the backfill on the seismic enactment of retaining walls. The results presented that the seismic load contrary to the retaining wall could be significantly reduced among the presented technique.

Most of the studies related to the liquid storage tanks that consider the soil effect is focused on fluid-structure-soil interaction and the effect of tank fixity conditions to the ground, while it was not found that any study dealt with the effect of hydrodynamic pressure on the soil behavior and soil parameters. Besides, the knowledge is insufficient about the influence of hydrodynamic pressure on saturated sand soil and its effect on the different sand relative densities. Due to these reasons, this study is devoted to considering the effect of hydrodynamic pressure in a liquid storage tank using different experimental methods for saturated sand density.

In this paper, the response of saturated soil supporting cylindrical water storage ground tanks under the hydrodynamic pressure is considered. The work targets specifically: (i) to investigate the influence of acceleration characteristics on the saturated sand has different relative densities; (ii) to investigate the potential settlement and lateral displacement of water tank under the influence of hydrodynamic pressure; and (iii) to investigate the excess pore pressure variation during an earthquake.

This paper has the following structure. Section 1 gives the previous studies related to the storage tank and hydrodynamic pressure. Section 2 describes the methodology and experimental investigation, including the shake table and soil properties. Section 3 describes the test preparation for controlling sand density. Section 4 illustrates the test program and flowchart for the shake table test. Section 5 implements earthquake data used in the tests. Section 6 introduces and discusses experimental test results. Finally, the conclusion of the work is presented in section 7. Figure 1 presents a flowchart of the research methodology used in this study.

2. EXPERIMENTAL INVESTIGATION

2. 1. Soil Properties Diyala Black Sand is used in the experimental work, and several tests are performed with two relative densities (medium with Dr = 50% and dense with 75%). The conducted soil tests are carried out according to ASTM standards. According to USCS, the sand was poorly graded, and the properties resulting from the implemented tests with the used standard methods on the sand are summarized in Table 1.

2. 2. Shake Table The shake table used in this study was fabricated according to instructions given by Al-Omari et al. [11]. The shake table simulates the earthquake condition to investigate the model's performance with high quality, reliability, and cost-efficiency, as shown in Figure 2. In the current study, due to the huge dimensions of the full-scale model for liquid storage tank with height of 10m and diameter of 14m, and the available container of the shear box with

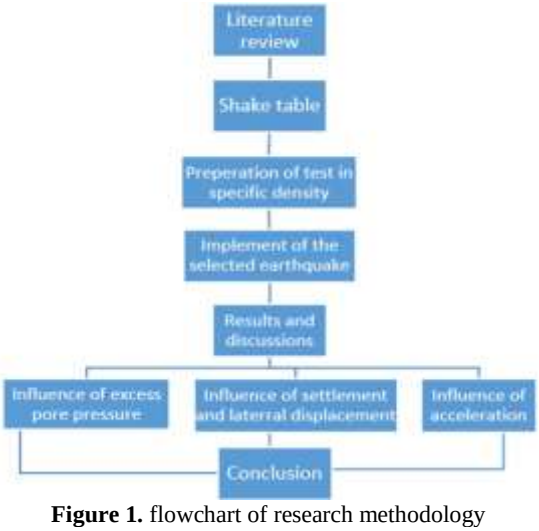

Figure 1. flowchart of research methodology

TABLE 1. physical properties and tests carried out on soils with standards

Soil Property	Medium Sand	Dense Sand	Standard
Relative density Dr(%)	50	75	
Max. γ_d (kN/m^3)	19.25		ASTM D4253
Min. γ_d (kN/m^3)	16.41		ASTM D4254
γ_d (kN/m^3)	17.72	18.64	
γ_{Total} (kN/m^3)	22.68	23.3	
Wc (%)	28	25	ASTM D2216
G.s	2.66		ASTM D854
Effective size D_{10}	0.145		
Effective size D_{30}	0.277		
Effective size D_{60}	1.675		ASTM D422
uniform Coefficient, Cu	11.5		
curvature Coefficient, Cc	0.315		
Soil classification USCS	Poorly graded sand		ASTM D2487
Soil color	Pale black		
Friction angle, deg.	30	34	ASTM D2434

dimensions of 600×600×800 mm, the maximum dimension used in the container is 150mm to verify the stress bulb zone's size. The tank model with a diameter of 140mm and a height of 100mm, which means the (1:100) scale factor has been used. The cylindrical storage tank model was filled with water up to 80 mm was placed at the center of the soil surface. However, a flexible laminar shear box has been used to reduce the reflection of seismic energy.

3. TEST PREPARATION

Several methods controlling sand density were attempted to prepared air-dried sand. Dry tamping was the preferred method since it ensured an extensive range of relative densities, on the antithesis of air pluvial or vibration methods which their results were limited to the (very loose-loose) range for the utilized sand. Two relative densities (50 and 75) % were performed to consider the influence of sand density on liquefaction potential. The calibration for both relative densities was performed utilizing maximum/minimum density mold with the volume of 0.0027 m^3; the sand layer was tamped utilizing a hammer with the weight of 86 N and released freely from a height of 75 mm. Table 2 summarizes the calibration of the density for each density required and the resultant energy of tamping for mold that was considered in Equation (1).

Figure 2. Fixable laminar shear box installed on the table

Energy/Volume=(hammer weight× drop height of hammer× blows number per layer× layer number)/ (Mold volume) (1)

In order to obtain tamping energy for the test model similar to that of the calibration mold, the sand layer was divided into layers of equal thickness of 100 mm for each layer then tamped to achieve the required relative density (50% and 75%). Similarly, the hammer with an area of 0.0179 m^2 was utilized that covers mostly 100% of the calibration mold area. Thus to tamp about 100% of the model sand area that was 0.36 m^2 which is 20.1 times, the hammer area of about 20 blows is needed to ensure that the tamping is covered most of the sand area. Two different layouts of 20 blow tamping passes were selected to ensure that the tamping effort was equally distributed through each layer. The energy of tamping for the test model was calculated again by utilizing Equation (1) and the values are reported in Table 3 that presents evidence for equivalents tamping energy for calibration mold and test model.

Finally, a relation between the tamping energy for controlling density against a relative density for both the test model and calibrated model were plotted in Figure 3.

The sand was air-dried and poured inside the storage barrel; after that, tamped in layers to obtain the required density. To study the influence of liquid storage tanks on soil density, three cases of soil layer configurations

TABLE 2. The studied cases of acceleration history

Relative density (%)	50	75
Count of blows per layer	1	3
Thickness of layer (mm)	50	50
Number of layers	3	3
Hammer weight (N)	86	86
Drop Height of hammer (mm)	75	75
Mold volume (m^3)	0.002686	0.002686
Energy (N.m)	19.35	58.05
Energy per volume (kN.m/m^3)	7.204	21.61

TABLE 3. The studied cases of acceleration history

Relative density (%)	50	75
blows number per layer	40	120
Thickness of layer (mm)	100	100
Number of layers	6	6
Hammer weight (N)	86	86
Drop Height of hammer (mm)	75	75
Mold volume (m^3)	0.216	0.216
Energy (N.m)	1548	4644
Energy per volume ($kN.m/m^3$)	7.16	21.5

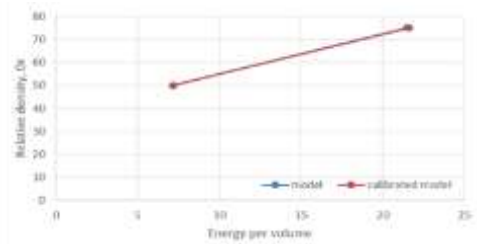

Figure 3. The relation between tamping energy against relative density for test model and calibrated model

are selected. These cases of the soil profile, as illustrated in Figure 4 are consist of the single medium layer of sand with a relative density of (50%) and 600 mm thickness, a dense layer with a relative density of (75%) and a third one consists of two layers of the sand, the top layer is medium sand (50% Dr.), and the lower layer is dense sand (75% Dr.) with a thickness of 300 mm for each layer.

The pore pressure transducers and accelerometers were embedded during the preparation of sand layers at three depths (140, 280, and 560) mm; the test model layout l is shown in Figure 5. After the soil profile was formed, the storage tank was placed at the center of the soil surface, and three displacement transducers were linked to the center of the storage tank across a screw nut.

4. TESTING PROGRAM FOR SHAKE TABLE TESTS

Six shake table tests were conducted on different soil densities. For more clarification, the testing program

Figure 4. Cases of study of a soil profile

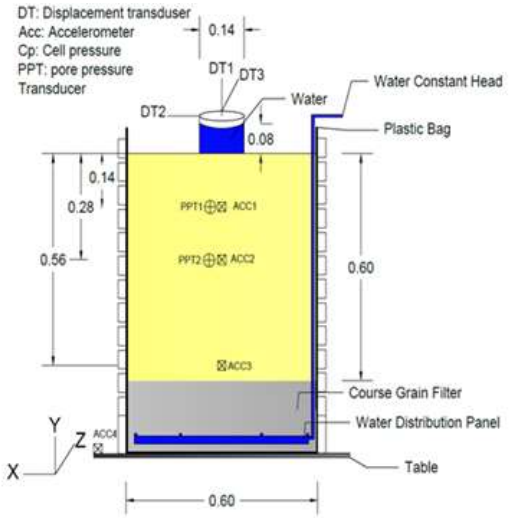

Figure 5. Test model layout

was illustrated in a flowchart in Figure 6. The test program was divided into two major parts; the first one used a water storage tank with a water height of (80mm) to represent the storage tank in case of hydrodynamic pressure. Furthermore, the other tank was filled with an equivalent load to represent the tank without hydrodynamic pressure.

5. IMPLEMENTATION OF EARTHQUAKE DATA

To study the effects of a wide range of acceleration characteristics on the saturated sandy soil, various real earthquake acceleration history data were implemented on models. The real acceleration histories for Ali Al-Gharbi, El-Centro, and Kobe were utilized. The calibration for the shake table was performed for these earthquakes by comparing the input acceleration by considering the full weight of the container and output acceleration during the earthquake, which presented very good compatibility. Table 4 summarizes information for earthquake data. Furthermore, due to the

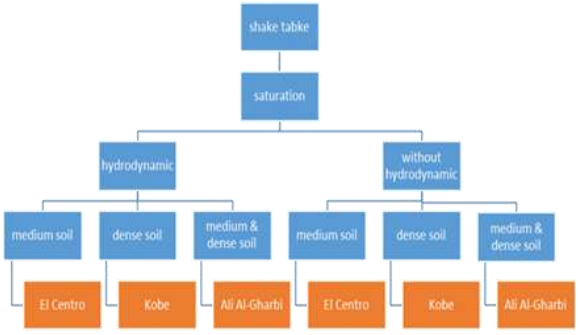

Figure 6. Flowchart for shake table test

TABLE 4. The studied cases of acceleration history

Acceleration History	Duration (s)	Acceleration Factor	Max. acceleration (g)
Ali Al-Gharbi	90	4.0	0.4
El-Centro	35	1.0	0.35
Kobe	30	1.0	0.82

small value of the maximum acceleration of the Ali Al-Gharbi earthquake (0.1g) and the significant scale factor (1:100), this acceleration has been amplified by multiplying it with four acceleration factors to impact the results in all studied cases.

6. RESULTS AND DISCUSSIONS

Test results have presented as relationships form between the various parameters studied against the time, including the acceleration, tank settlement, lateral displacement, and excess pore pressure distributed within three depths in the soil layer (140mm, 280mm, and 560mm) as illustrated in Figure 5. These parameters were obtained using the earthquake shake table accelerometer, displacement transducer, and pore water pressure transducer. Besides, the values of the settlement, the lateral displacement in (X and Z)-directions (where the X in the direction corresponding to the input acceleration direction and the Z is the direction perpendicular to the X) were presented in Figures 7 to 12.

6. 1. Influence of Earthquake History The results of these tests were presented in Figures 7 and 8. Generally, the earthquake acceleration inside the soil is less than the input acceleration at the table level. The acceleration at the bottom-depth of the soil column is

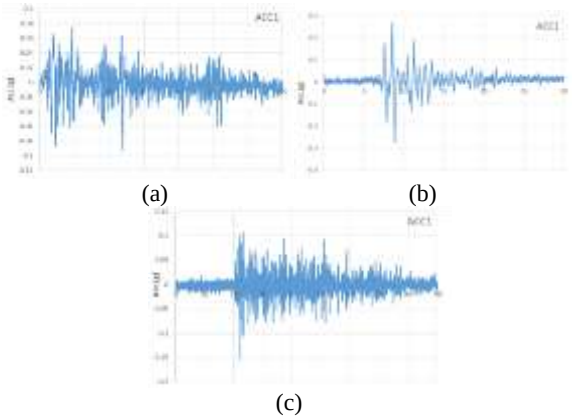

(a) (b)

(c)

Figure 7. Results of Acceleration in depth (140mm) in case of Hydrodynamic pressure for (a) El-Centro, (b) Kobe, and (c) Ali Al-Gharbi earthquake

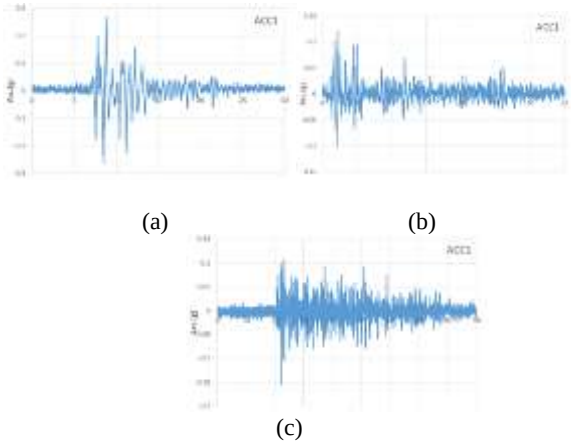

(a) (b)

(c)

Figure 8. Results of Acceleration in depth (140mm) in case of without Hydrodynamic pressure for (a) El-Centro, (b) Kobe, and (c) Ali Al-Gharbi earthquake

slightly higher than at the mid-depth, while in the top portion of the soil column, the acceleration is comparatively less than that at the mid-depth due to saturated soil damping and acceleration spread out throughout the soil matrix. Figure 9 presents the variation of maximum acceleration with a depth in hydrodynamic pressure for all earthquakes. This finding seems to be consistent with Su et al. [13]. Earthquake frequencies significantly increased in the bottom depth and reduction in the top depth near the soil surface.

6. 2. Influence of Settlement and Lateral Displacement In all acceleration history cases, the settlement in the hydrodynamic pressure of the liquid storage tank was significantly increased compared to results of without-hydrodynamic pressure influenced by the hydrodynamic pressure onto the tank wall that is turned to the tank base applying additional forces. As a result, an additional settlement has occurred, as is presented in Figure 10. The storage tank settlement for the Ali Al-Gharbi earthquake was started at 22 seconds and increased as the pore water pressure

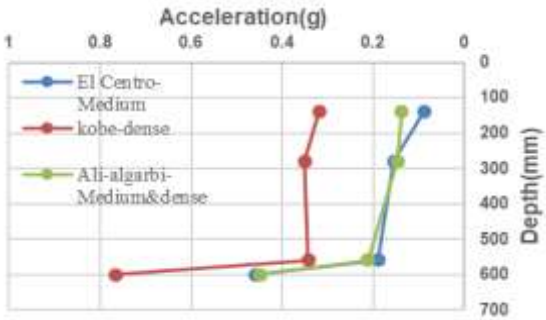

Figure 9. Variation of maximum acceleration with depth for El-Centro, Kobe, and Al Al-Gharbi in case of a liquid storage tank

generated, continued to increase, after 75 seconds, the storage tank settlement diminished at 0.063D and 0.059D (where D is the diameter of the storage tank) in case of with and without hydrodynamic pressure, respectively. In the El-Centro earthquake, it is observed that the storage tank settlement is about 0.025D and 0.024D in the case of with and without hydrodynamic pressure, respectively. The storage tank settlement in the Kobe earthquake is 0.091D and 0.08D in case of with and without hydrodynamic pressure, respectively; which they take place between 8 second and 30 seconds of earthquake duration as the generation of excess pore water pressure started that showed a noticeable effect of liquefaction.

Figure 11 displays the influence of hydrodynamic pressure on the soil settlement for cases of (El-Centro, Ali Al-Gharbi, and Kobe), it can be concluded that the increment in settlement for hydrodynamic pressure of saturated sand in the case of El-Centro is 3.2%, and 6.2% is the increment in Ali Al-Gharbi. In comparison, an increase in Kobe was 13.2% from the case without hydrodynamic pressure. Also, it was noticed that the effect of hydrodynamic pressure in the Kobe earthquake was higher than El-Centro and Ali Al-Gharbi acceleration earthquakes.

In addition, the final displacement in x- and y-directions was calculated in both cases as illustrated in Table 5. It was found that the lateral displacement of hydrodynamic pressure in Kobe was increased by 121%, 11.5% for Ali Al-Gharbi, and 101% for the El-Centro earthquake in the case of without hydrodynamic pressure. The lateral displacement in z-direction for three earthquakes of with and without hydrodynamic pressure exhibited an increment with 297%, 214%, and 143% in El-Centro, Kobe, and Ali Al-Gharbi earthquakes acceleration, respectively. Also, it was found that the soil density affects the hydrodynamic pressure value, which later influences the displacement results. In all soil densities, the settlement and lateral displacement in the z-direction increase with an increase of the acceleration amplitude and shaking duration.

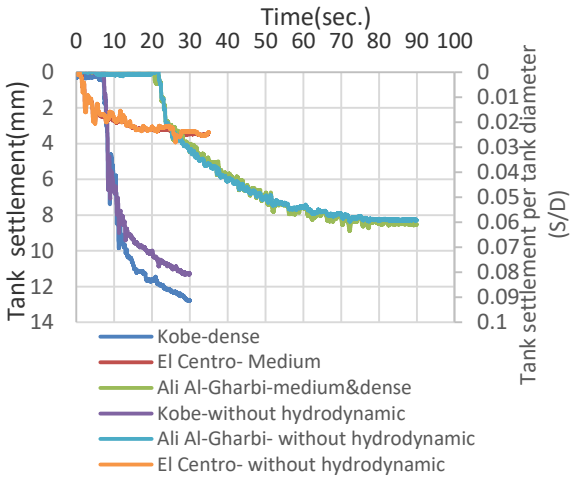

Figure 10. Results of settlement for all cases with hydrodynamic pressure and without Hydrodynamic pressure

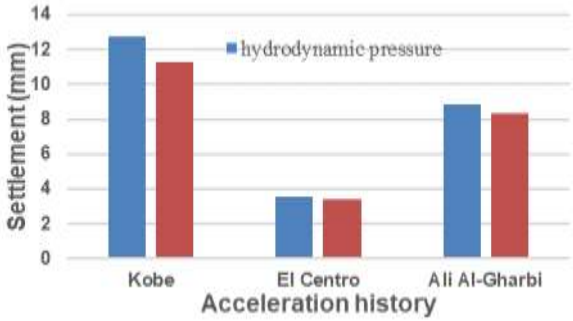

Figure 11. Variation of maximum settlement in hydrodynamic pressure and without hydrodynamic pressure for three earthquake histories

TABLE 5. Final lateral displacement in the x-direction for hydrodynamic pressure and without hydrodynamic pressure in three earthquake histories

Acceleration History	El-Centro	Kobe	Ali Al-Gharbi
x-displacement (hydrodynamic pressure)	1.05	4.2	2.9
x-displacement (without hydrodynamic pressure)	0.52	1.9	2.6
z-displacement (hydrodynamic pressure)	3.3	2.2	2.17
z-displacement (without hydrodynamic pressure)	0.83	0.7	0.89

6. 3. Influence of Excess Pore Pressure

When the earthquake hits saturated sand, the pore pressure was suddenly raised to a high value within a short time that disables drainage immediately, no matter how high the permeability of sand is. Sand particles cannot withstand this increase in pore pressure; hence, their contacts are lost, and the shear strength is significantly reduced; this is known as a liquefying stage. Following that, as it is known, the fluid flows across high pressures into low-pressure areas; therefore, accumulated pore water pressure flows upward towards the low-pressure region at the surface to neutralize the fluid pressure; this stage is known as a dissipation stage. During this stage, the soil particles are relatively moved downward due to the action of shaking to fill the voids of the dissipated water and recover strength as the contact between particles was re-established; thus, densification of sand occurred at the end of the shaking duration. In particular, the influences of the relative density of the soil have been considered. It controls the soil's tendency to contract or dilate upon shear, and

therefore the nature of excess pore pressure may develop in the soil. In the Ali Al- Gharbi earthquake, the initial liquefaction does not occur in both depths; the pore water pressure starts to generate rapidly at 22 seconds of acceleration duration, at both soil layers (top and bottom) in the case of hydrodynamic pressure (Excess Pore pressure Ratio) EPR reaches to (0.55, and 0.49), respectively.

In the same way, EPR reaches (0.55,0.37) at the top and bottom soil layer in the case without hydrodynamic pressure. In the El-Centro earthquake, pore water pressure generation shows no significant liquefaction effects on the tested soil and start to initiate after approximately 3 seconds, EPR in case of hydrodynamic pressure reaches (0.49, 0.39) at the upper and lower of the soil layer, respectively; while EPR reaches (0.61, 0.48) in case of without hydrodynamic pressure at top and bottom of soil layer, respectively. In the Kobe earthquake, the pore pressure increases sharply after 7 seconds, and EPR reaches the initial liquefaction at the top of the soil layer in both cases of hydrodynamic and without hydrodynamic pressure, while EPR reaches (0.95, 0.91) at the bottom depth of soil in both cases hydrodynamic and without hydrodynamic pressure, respectively. The idea of Keefer [13] and Rodriguez et al. [14], which is the shaking threshold that is needed to produce liquefaction are earthquake acceleration magnitude larger than M=5, supports these findings. Figure 12 illustrates the difference between the maximum (EPR) in the case of hydrodynamic pressure and without hydrodynamic pressure in the top and bottom states for three earthquake acceleration histories. In the case of the Kobe earthquake, liquefaction occurred at the top in both cases, and the EPR2 in hydrodynamic pressure was increased by 4% without hydrodynamic pressure. EPR1 in the Ali Al Gharbi earthquake was presented similar results and an increment in hydrodynamic pressure with 32% in EPR2 compared to the case without hydrodynamic pressure. On the contrary, the El-Centro earthquake (EPR1) and (EPR2) were decreased by (24%) and (23%), respectively in the case of hydrodynamic pressure.

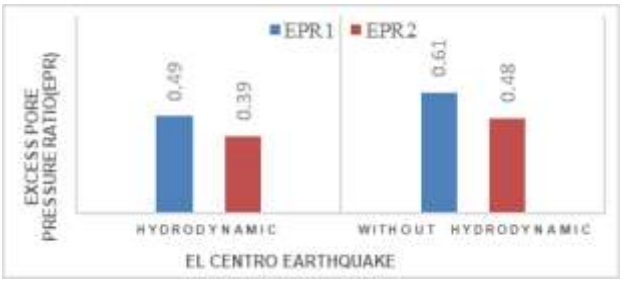

(a)

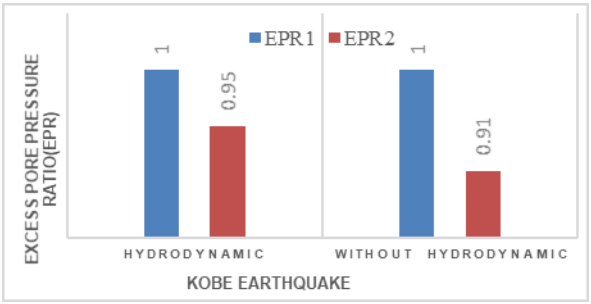

(b)

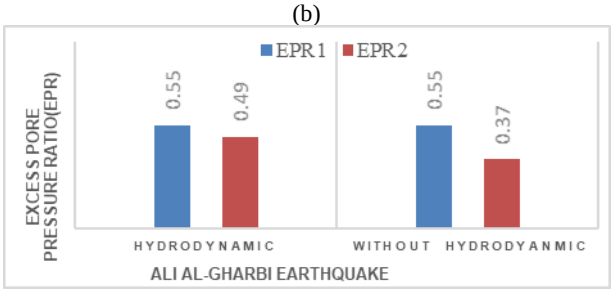

(c)

Figure 12. Variation of maximum excess pore pressure ratio (EPR) in hydrodynamic pressure and without hydrodynamic pressure for (a) El-Centro, (b) Kobe, and (c) Ali Al-Gharbi earthquake

7. CONCLUSIONS

In this paper, experimental shake table tests consider the influence of hydrodynamic pressure performed on saturated sandy soil loaded by cylindrical storage tanks during three earthquake histories. From the analysis of the results, the hydrodynamic pressure was concluded to significantly influence the saturated soil settlement and increased with (3.2%, 6.2%, and 13.2%) for El-Centro, Ali Al Gharbi, and Kobe respectively of without hydrodynamic pressure state. A lateral displacement was also influenced by the hydrodynamic pressure; in the x-direction, the increment in the hydrodynamic pressure state's displacement was (121%, 101%, and 11.5%) in Kobe, El-Centro, and Ali Al-Gharbi, respectively of without hydrodynamic pressure state. Likewise, in the hydrodynamic pressure state, the z-direction displacement was increased, 214%, 297%, and 143% in Kobe, El-Centro, and Ali Al Gharbi, respectively of without a hydrodynamic pressure state. Excess pore pressure was monitored and exhibited an increment in the Kobe earthquake, the liquefaction occurred at the EPR1 in both cases, and the EPR2 in hydrodynamic pressure was increased 4% in the case of without hydrodynamic pressure. EPR1 in the Ali Al-Gharbi earthquake is the same in results, and the increment in hydrodynamic pressure is 32% in EPR2 compared to the case without hydrodynamic pressure. On the contrary, the hydrodynamic pressure state of El-

Centro earthquake (EPR1) and (EPR2) were decreased by (24%) and (23%), respectively.

8. REFERENCES

1. Kianoush, M. and Ghaemmaghami, A. "The effect of earthquake frequency content on the seismic behavior of concrete rectangular liquid tanks using the finite element method incorporating soil–structure interaction". ***Engineering Structures***, Vol. 33, No. 7, (2011), 2186-2200, https://doi.org/10.1016/j.engstruct.2011.03.009
2. Chaduvula, U., Patel, D., and Gopalakrishnan, N. "Fluid-structure-soil interaction effects on seismic behaviour of elevated water tanks". ***Procedia Engineering***. Vol. 51, (2013), 84-91. https://doi.org/10.1016/j.proeng.2013.01.014.
3. Chaithra, M., Krishnamoorthy, A., and PM, N. N. "Analysis of soil-structure Interaction on response of tanks Filled with fluid". ***International Journal of Civil Engineering and Technology***, Vol. 8, No. 7, (2017), 813-819. http://www.iaeme.com/IJCIET/issues.asp?JType=IJCIET&VType=8&IType=7
4. Kotrasová, K. "Sloshing of liquid in rectangular tank". ***Advanced Materials Research***, Vol. 969, (2014), 320-323. https://doi.org/10.4028/www.scientific.net/AMR.969.320
5. Chougule, A. and Patil, P. "Study of seismic analysis of water tank at ground level". ***International Research Journal of Engineering and Technology,*** Vol. 4, No. 7, (2017), 2895-2900.
6. Sadek, E. S. A., Gomaa, M. S., and El Ghazaly, H. A. "Seismic behavior of ground rested rectangular RC tank considering fluid-structure-soil interaction", (2019), DOI: 10.9790/1684-1601010115.
7. Hussein, A. A., Al-Neami, M. A., and Rahil, F. H. "Hydrodynamic Pressure Effect of the Tank Wall on Soil–Structure Interaction". ***Modern Applications of Geotechnical Engineering and Construction***, (2021), 173-184. https://doi.org/10.1007/978-98115-4-9399.
8. Waghmare, M. V., Madhekar, S. N., and Matsagar, V. A. "Influence of Nonlinear Fluid Viscous Dampers on Seismic Response of RC Elevated Storage Tanks". ***Civil Engineering Journal***, Vol. 6, (2020), 98-118. DOI: 10.28991/cej-2020-SP(EMCE)-09.
9. Pan, H. and Jiang, X. "On the Characteristics of Ground Motion and the Improvement of the Input Mode of Complex Layered Sites". ***Civil Engineering Journal***. Vol. 6, No. 5, (2020), 848-859. DOI: 10.28991/cej-2020-03091512.
10. Dram, A., Benmebarek, S., and Balunaini, U" .Performance of Retaining Walls with Compressible Inclusions under Seismic Loading". ***Civil Engineering Journal***, Vol. 6, No. 12, (2020), 2474-2488. DOI: 10.28991/cej-2020-03091631.
11. Al-Omari, R. R., Al-Kifae, A. A., & Al-Tameemi, S. M. "Earthquake effect on single pile behavior with various factor of safety and depth to diameter ratio in liqufiable sand" ***International Journal of Civil Engineering and Technology***, Vol. 9, No. 4, (2018), 1253-1262. http://www.iaeme.com/IJCIET/issues.asp?JType=IJCIET&VType=9&IType=4
12. Su, D., Ming, H., and Li, X. "Effect of shaking strength on the seismic response of liquefiable level ground". ***Engineering Geology***, Vol. 166, (2013), 262-271. https://doi.org/10.1016/j.enggeo.2013.09.013.
13. Keefer, D. K. "Landslides caused by earthquakes". ***Geological Society of America Bulletin***, Vol. 95, No. 4, (1984), 406-421. https://doi.org/10.1130/0016-7606(1984)95<406:LCBE>2.0.CO;2.
14. Rodrıguez, C., Bommer, J., and Chandler, R. "Earthquake-induced landslides: 1980-1997". ***Soil Dynamics and Earthquake Engineering***. Vol. 18, No. 5, (1999), 325-346. https://doi.org/10.1016/S0267-7261(99)00012-3.

Persian Abstract

چکیده

این مقاله با هدف روشن کردن تأثیر فشار هیدرودینامیکی تولید شده در یک مخزن ذخیره آب بر رفتار شن اشباع شده از آن پشتیبانی می کند. آزمایشات بر روی دو مدل مخزن استوانه ای مخزن آب با استفاده از یک میز تکان دهنده ساخته شده که از یک جعبه برشی لایه ای انعطاف پذیر تشکیل شده است ، انجام شد. مدل اول یک مخزن ذخیره آب است که تا حدی پر از آب است و مدل دوم یک مخزن با بار معادل فشار آب برای شبیه سازی مخزن ذخیره آب بدون فشار هیدرودینامیکی است. سه تاریخ زلزله (کوبه ، ال-سانترو و علی الغربی) بر روی مدل ها برای بررسی دامنه متنوع شتاب اجرا شد. مشخص شد که جهت حل و فصل و جابجایی جانبی در مخزن ذخیره آب به طور قابل توجهی افزایش یافته است در مقایسه با بار معادل منجر به مدل دوم در تمام موارد از تاریخ شتاب است. همچنین ، فشار آب منافذ در طول دوره آزمایش کنترل شد ، و متوجه شدیم که فشار منفذی بیش از حد تحت تأثیر فشار هیدرودینامیکی قرار گرفته است که در مقایسه با نتایج ثبت شده در شرایط عدم فشار هیدرودینامیکی افزایش می یابد.